Vol 14 No 4, April 2005
1009-1963/2005/14(04)/0683-07

Chinese Physics

© 2005 Chin. Phys. Soc.
and IOP Publishing Ltd

Gravitational quasinormal modes of the Reissner–Nordström de Sitter black hole*

Jing Ji-Liang (荆继良)† and Chen Song-Bai(陈松柏)

Institute of Physics, Hunan Normal University, Changsha 410081, *China*

(Received 7 September 2004; revised manuscript received 8 December 2004)

By using the Pöschl–Teller potential approximation, the quasinormal modes of the Reissner–Nordström de Sitter black hole for the axial and polar gravitational perturbations are investigated. It is shown that the magnitude of imaginary part decreases as the cosmological constant increases, but it increases as the charge, or the overtone number or the orbital angular momentum increases. The imaginary part is almost linearly related to the real part as cosmological constant changes for a fixed charge. It is also found that the gravitational quasinormal modes are the same for both the axial and polar perturbations, which proves that the quasinormal modes are determined only by the parameters of the black hole and are independent of the initial perturbations.

Keywords: black hole, gravitational perturbation, quasinormal modes
PACC: 0470, 0450, 1115

1. Introduction

The dynamics of field perturbation in black hole spacetime has been studied for almost thirty years.[1,2] It is well-known that there are three stages of the dynamical evolution.[3] The initial wave burst is caused by the perturbation and the wave is dependent on the initial form of the perturbation, the damping oscillation, and the power-law tail behaviour of the wave at very late time which is caused by the backscattering of the gravitational field. The second stage, the damping oscillation or quasinormal ringing, can be accurately described in terms of the quasinormal modes (QNMs) which are defined as proper solutions of the perturbation equations belonging to certain complex characteristic frequencies which satisfy the boundary conditions suitable for purely ingoing waves at the horizon and purely outgoing waves at infinity.[4] It is believed that the QNM is a unique fingerprint in directly identifying the existence of black hole since its frequency and damping time are entirely fixed by the structure of the background spacetime and are independent of the initial perturbation. The detection of the QNM is expected to be realized through gravitational wave observation.

Since Regge and Wheeler[5] first presented the idea of the QNM and Chandrasekhar and Detweller[4] worked out the numerical calculation of the QNM for the asymptotically flat Schwarzschild black hole, a great deal of effort has been devoted to computing the QNM of the asymptotically flat spacetime.[1,2,6–12] The QNM in asymptotically flat spacetime has recently received much attention since the real part of the quasinormal frequency with its large imaginary part is equal to the value of the Barbero–Immirzi parameter.[13,14]

Recently, many authors have delved into the QNMs for black holes in the asymptotically anti-de Sitter space (AdS)[15–26] since a large static black hole in AdS spacetime corresponds to a (approximately) thermal state in the conformal field theory (CFT) and the decay of the test field in the spacetime of the black hole corresponds to the decay of the perturbed state in CFT. Perturbing the black hole is equivalent to perturbing this thermal state, and the decay of the perturbation describes the return to the thermal equilibrium. Therefore, we can obtain a prediction for the thermalization time scale in the strongly coupled

*Project supported by the National Natural Science Foundation of China (Grant No 10275024), the Foundation for Author of National Excellent Doctoral Dissertations of China (Grant No 200317), and the Hunan Provincial Natural Science Foundation of China (Grant No 04JJ3019).

†E-mail: jljing@hunnu.edu.cn

CFT.

The QNM of the black hole in asymptotically de Sitter (dS) spacetime has attracted much attention recently[27−33] due to the observed evidence that our universe has a positive cosmological constant.[34−36] The QNM frequencies for gravitational perturbations of the Schwarzschild dS black hole were first worked out by Moss and Norman.[27] By using the analytical approximation method Cardoso and Lemos[28] studied the QNM for the case in which the black hole and cosmological horizons are very close to each other. The analytical approximation method was also applied by Molina[29] to QNM of higher dimensional Schwarzschild dS black holes, and by Maassen[30] to the QNMs for the scalar, electromagnetic, and gravitational fields of the Schwarzschild dS black hole. By applying the WKB and Pöschl–Teller potential approximation Zhidenko[33] calculated the QNM frequencies of the Schwarzschild–de Sitter black hole for scalar, electromagnetic, Dirac, and gravitational fields. Considering that the Reissner–Nordström de Sitter spacetime provides a better framework than the Schwarzschild dS geometry and may contribute significantly to our understanding of the QNMs, we[37] recently studied the quasinormal modes of the Reissner–Nordström de Sitter black hole for the massless Dirac field by using the Pöschl–Teller potential approximation. The main purpose of the paper is to extend the investigation to the gravitational QNM frequencies of the Reissner–Nordström de Sitter black hole due to the axial and polar gravitational perturbations.

In the next section, the quasinormal mode frequencies of the Reissner–Nordström de Sitter black hole for the axial and polar gravitational perturbations are calculated by using the Pöschl–Teller potential approximation and the results are presented in tables and figures. The last section is devoted to discussion and conclusions.

2. Gravitational quasinormal mode frequencies in Reissner–Nordström de Sitter black-hole spacetime

The metric for the Reissner–Nordström de Sitter black hole in standard coordinates can be written as

$$\mathrm{d}s^2 = -f\mathrm{d}t^2 + \frac{1}{f}\mathrm{d}r^2 + r^2(\mathrm{d}\theta^2 + \sin^2\theta\mathrm{d}\varphi^2), \quad (1)$$

with

$$f = 1 - \frac{2M}{r} + \frac{Q^2}{r^2} - \frac{\Lambda}{3}r^2, \quad (2)$$

where the parameters M, Q, and Λ represent the black hole mass, the charge, and the cosmological constant, respectively.

In the analysis of the black hole stability to gravitational perturbations, Mellor and Moss[38] have found that, for both the axial and polar perturbations, the decoupled equations can be expressed as

$$\frac{\mathrm{d}^2\Psi}{\mathrm{d}r_*^2} + (\omega^2 - V_i)\Psi = 0, \quad (3)$$

where r_* is the "tortoise" coordinate

$$r_* = \int \frac{\mathrm{d}r}{f}, \quad (4)$$

and V_i are the potentials (V_1 is for the axial perturbation, and V_2 for the polar perturbation), which are explicitly given by

$$V_1 = \frac{f}{r^4}[l(l+1)r^2 - \sqrt{9M^2 + 4Q^2(l-1)(l+2)}r - 3Mr + 4Q^2], \quad (5)$$

$$V_2 = \frac{f}{r^3}[U - \sqrt{9M^2 + 4Q^2(l-1)(l+2)}W], \quad (6)$$

with

$$U = \{[l(l+1)-2]r + 3M\}W + \left\{\frac{[l(l+1)-2]r}{2} - \frac{2Q^2}{r} - \frac{1}{2}[l(l+1)-2]r + 2M - \frac{2}{3}\Lambda r^3\right\} - \frac{[l(l+1)-2]r^2 f}{[l(l+1)-2]r/2 + 3M - 2Q^2/r}, \quad (7)$$

$$W = \frac{rf\{[l(l+1)-2]r + 3M\}}{[[l(l+1)-2]r/2 + 3M - 2Q^2/r]^2} + \frac{[l(l+1)-2]r/2 + M + 2\Lambda r^3/3}{[l(l+1)-2]r/2 + 3M - 2Q^2/r}. \quad (8)$$

In Ref.[27] Moss and Norman have proved that the gravitational QNMs of the Schwarzschild–de Sitter black holes obtained by Leaver approach[39] are in agreement with the results obtained in the Pöschl–Teller approximation for the low overtone. In Ref.[33] Zhidenko has shown that the quasinormal modes obtained respectively in the Pöschl–Teller approximation and WKB approximation are in good agreement with each other for the Schwarzschild–de Sitter black holes. The reason for the results obtained in the Pöschl–Teller potential approximation being in good agreement with other numerical results is that the scattering potential of black hole in the de Sitter space

falls off exponentially. Therefore, we can calculate the gravitational quasinormal mode of the Reissner–Nordström de Sitter black hole by using Pöschl–Teller approximate potential[40]

$$V_{\mathrm{PT}} = \frac{V_0}{\cosh^2(r_*/b)}. \tag{9}$$

The potential contains two free parameters (V_0 and b) which are used to fit the height and the second derivative of the potential V_1 and V_2 at the maximum. The QNM frequencies of the Pöschl–Teller potential can be evaluated analytically, which are given by

$$\omega_n = \frac{1}{b}\left[\sqrt{V_0 b^2 - \frac{1}{4}} - \left(n + \frac{1}{2}\right) i\right]. \tag{10}$$

However, the quantities V_0 and b for different values of Q and Λ should be found numerically. The gravitational quasinormal mode frequencies of the Reissner–Nordström de Sitter black hole for different perturbations and different values of the Q, Λ, l, and n obtained by using the Pöschl–Teller potential approximation are presented in tables and figures below. Tables 1–3 and Figs.1–3 describe the case of the axial perturbation, i.e. for the potential (5).

Table 1. Gravitational quasinormal mode frequencies for the axial approximation: $l = 2$.

				n=0			
ω	Q=0.0	Q=0.1	Q=0.2	Q=0.3	Q=0.4	Q=0.5	Q=0.6
$\Lambda = 0.00$	0.3783–0.0905i	0.3785–0.0906i	0.3793–0.0906i	0.3808–0.0908i	0.3830–0.0910i	0.3862–0.0912i	0.3907–0.0914i
$\Lambda = 0.02$	0.3416–0.0830i	0.3420–0.0831i	0.3433–0.0834i	0.3450–0.0835i	0.3479–0.0839i	0.3520–0.0844i	0.3576–0.0850i
$\Lambda = 0.04$	0.3010–0.0742i	0.3015–0.0743i	0.3029–0.0746i	0.3055–0.0751i	0.3092–0.0757i	0.3145–0.0766i	0.3214–0.0775i
$\Lambda = 0.06$	0.2545–0.0636i	0.2551–0.0638i	0.2572–0.0642i	0.2606–0.0649i	0.2656–0.0660i	0.2724–0.0673i	0.2812–0.0688i
$\Lambda = 0.08$	0.1980–0.0502i	0.1990–0.0504i	0.2019–0.0511i	0.2069–0.0522i	0.2139–0.0538i	0.2231–0.0558i	0.2349–0.0582i
$\Lambda = 0.09$	0.1629–0.0415i	0.1642–0.0418i	0.1679–0.0428i	0.1742–0.0443i	0.1829–0.0463i	0.1942–0.0489i	0.2082–0.0520i
$\Lambda = 0.10$	0.1180–0.0303i	0.1199–0.0307i	0.1253–0.0321i	0.1340–0.0343i	0.1457–0.0371i	0.1602–0.0406i	0.1776–0.0446i
$\Lambda = 0.11$	0.0373–0.0096i	0.0430–0.0110i	0.0570–0.0147i	0.0750–0.0193i	0.0952–0.0244i	0.1171–0.0299i	0.1408–0.0356i
				n=1			
$\Lambda = 0.00$	0.3783–0.2716i	0.3785–0.2717i	0.3793–0.2718i	0.3808–0.2723i	0.3833–0.2729i	0.3862–0.2735i	0.3907–0.2741i
$\Lambda = 0.02$	0.3416–0.2490i	0.3420–0.2492i	0.3431–0.2497i	0.3450–0.2506i	0.3479–0.2518i	0.3520–0.2532i	0.3576–0.2548i
$\Lambda = 0.04$	0.3010–0.2226i	0.3015–0.2229i	0.3029–0.2239i	0.3055–0.2252i	0.3092–0.2271i	0.3145–0.2296i	0.3214–0.2326i
$\Lambda = 0.06$	0.2545–0.1908i	0.2551–0.1913i	0.2572–0.1926i	0.2606–0.1948i	0.2656–0.1979i	0.2724–0.2018i	0.2812–0.2064i
$\Lambda = 0.08$	0.1980–0.1504i	0.1990–0.1511i	0.2019–0.1532i	0.2069–0.1567i	0.2139–0.1615i	0.2231–0.1675i	0.2349–0.1747i
$\Lambda = 0.09$	0.1629–0.1246i	0.1642–0.1255i	0.1679–0.1283i	0.1742–0.1328i	0.1830–0.1390i	0.1942–0.1467i	0.2082–0.1558i
$\Lambda = 0.10$	0.1180–0.0908i	0.1198–0.0922i	0.1253–0.0963i	0.1340–0.1028i	0.1457–0.1114i	0.1602–0.1219i	0.1776–0.1338i
$\Lambda = 0.11$	0.0373–0.0289i	0.0430–0.0333i	0.0570–0.0441i	0.0750–0.0579i	0.0952–0.0733i	0.1171–0.0897i	0.1408–0.1066i

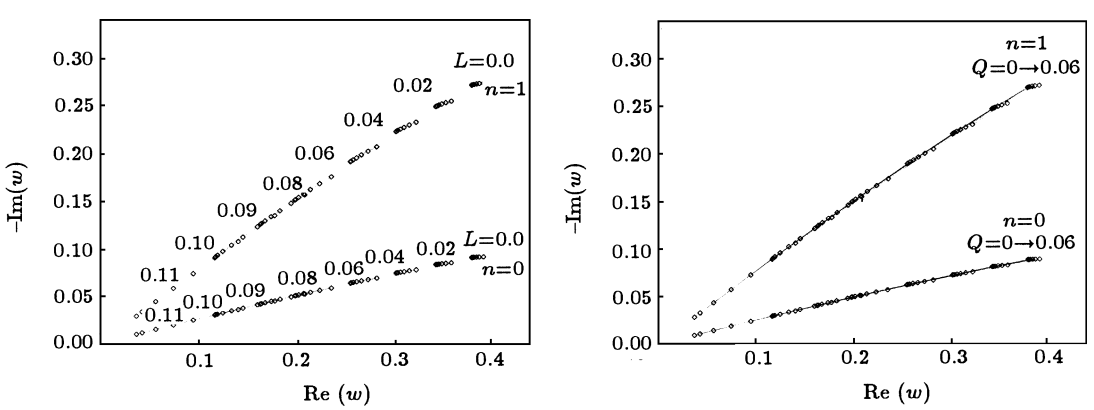


Fig.1. Gravitational QNMs for the axial perturbation: $l = 2$. In the left figure the curves are drawn for $\Lambda = L$ =0, 0.02, 0.04, 0.06, 0.08, 0.09, 0.10, 0.11, and in the right figure the curves are drawn for Q=0, 0.1, 0.2, 0.3, 0.4, 0.5, 0.6.

Table 2. Gravitational quasinormal mode frequencies for the axial perturbation: $l = 3$.

ω	Q=0.0	Q=0.1	Q=0.2	Q=0.3	Q=0.4	Q=0.5	Q=0.6
				n=0			
$\Lambda = 0.00$	0.6024–0.0934i	0.6028–0.0934i	0.6040–0.0935i	0.6063–0.0936i	0.6100–0.0937i	0.6156–0.0939i	0.6236–0.0941i
$\Lambda = 0.02$	0.5453–0.0851i	0.5458–0.0851i	0.5475–0.0853i	0.5506–0.0855i	0.5554–0.0859i	0.5623–0.0864i	0.5722–0.0869i
$\Lambda = 0.04$	0.4815–0.0755i	0.4822–0.0756i	0.4845–0.0759i	0.4886–0.0764i	0.4949–0.0771i	0.5036–0.0779i	0.5155–0.0789i
$\Lambda = 0.06$	0.4080–0.0644i	0.4091–0.0645i	0.4123–0.0650i	0.4178–0.0657i	0.4260–0.0668i	0.4373–0.0681i	0.4521–0.0697i
$\Lambda = 0.08$	0.3182–0.0505i	0.3197–0.0507i	0.3244–0.0515i	0.3324–0.0526i	0.3438–0.0542i	0.3591–0.0563i	0.3785–0.0587i
$\Lambda = 0.09$	0.2621–0.0417i	0.2641–0.0420i	0.2701–0.0430i	0.2802–0.0445i	0.2943–0.0466i	0.3128–0.0492i	0.3358–0.0523i
$\Lambda = 0.10$	0.1901–0.0303i	0.1930–0.0308i	0.2017–0.0322i	0.2158–0.0344i	0.2347–0.0373i	0.2584–0.0408i	0.2869–0.0448i
$\Lambda = 0.11$	0.0601–0.0096i	0.0694–0.0111i	0.0919–0.0147i	0.1209–0.0193i	0.1536–0.0245i	0.1892–0.0299i	0.2278–0.0357i
				n=1			
$\Lambda = 0.00$	0.6024–0.2801i	0.6028–0.2802i	0.6040–0.2804i	0.6063–0.2807i	0.6100–0.2811i	0.6156–0.2817i	0.6236–0.2822i
$\Lambda = 0.02$	0.5453–0.2551i	0.5458–0.2553i	0.5475–0.2558i	0.5506–0.2566i	0.5554–0.2577i	0.5623–0.2592i	0.5720–0.2608i
$\Lambda = 0.04$	0.4815–0.2266i	0.4822–0.2269i	0.4845–0.2278i	0.4886–0.2292i	0.4949–0.2312i	0.5036–0.2337i	0.5155–0.2367i
$\Lambda = 0.06$	0.4080–0.1932i	0.4091–0.1936i	0.4123–0.1950i	0.4178–0.1972i	0.4260–0.2003i	0.4373–0.2043i	0.4521–0.2091i
$\Lambda = 0.08$	0.3182–0.1515i	0.3197–0.1522i	0.3244–0.1544i	0.3324–0.1579i	0.3438–0.1629i	0.3591–0.1689i	0.3785–0.1762i
$\Lambda = 0.09$	0.2621–0.1251i	0.2641–0.1261i	0.2701–0.1289i	0.2802–0.1335i	0.2943–0.1399i	0.3129–0.1476i	0.3358–0.1569i
$\Lambda = 0.10$	0.1901–0.0910i	0.1930–0.0924i	0.2017–0.0965i	0.2158–0.1031i	0.2347–0.1118i	0.2584–0.1223i	0.2869–0.1344i
$\Lambda = 0.11$	0.0601–0.0289i	0.0694–0.0333i	0.0919–0.0441i	0.1209–0.0580i	0.1536–0.0734i	0.1892–0.0898i	0.2278–0.1071i
				n=2			
$\Lambda = 0.00$	0.6024–0.4669i	0.6028–0.4670i	0.6040–0.4673i	0.6063–0.4678i	0.6100–0.4686i	0.6156–0.4695i	0.6236–0.4702i
$\Lambda = 0.02$	0.5453–0.4252i	0.5458–0.4254i	0.5475–0.4263i	0.5506–0.4276i	0.5554–0.4296i	0.5623–0.4320i	0.5720–0.4346i
$\Lambda = 0.04$	0.4815–0.3777i	0.4822–0.3782i	0.4845–0.3796i	0.4886–0.3820i	0.4949–0.3853i	0.5036–0.3895i	0.5155–0.3945i
$\Lambda = 0.06$	0.4080–0.3220i	0.4091–0.3227i	0.4123–0.3250i	0.4178–0.3287i	0.4260–0.3339i	0.4373–0.3405i	0.4521–0.3484i
$\Lambda = 0.08$	0.3182–0.2525i	0.3197–0.2537i	0.3244–0.2573i	0.3324–0.2631i	0.3438–0.2712i	0.3591–0.2815i	0.3785–0.2937i
$\Lambda = 0.09$	0.2621–0.2086i	0.2641–0.2101i	0.2701–0.2148i	0.2802–0.2224i	0.2943–0.2329i	0.3128–0.2460i	0.3358–0.2614i
$\Lambda = 0.10$	0.1901–0.1517i	0.1930–0.1540i	0.2017–0.1609i	0.2158–0.1719i	0.2347–0.1863i	0.2584–0.2039i	0.2869–0.2241i
$\Lambda = 0.11$	0.0601–0.0481i	0.0694–0.0555i	0.0919–0.0735i	0.1209–0.0966i	0.1536–0.1223i	0.1892–0.1497i	0.2278–0.1785i

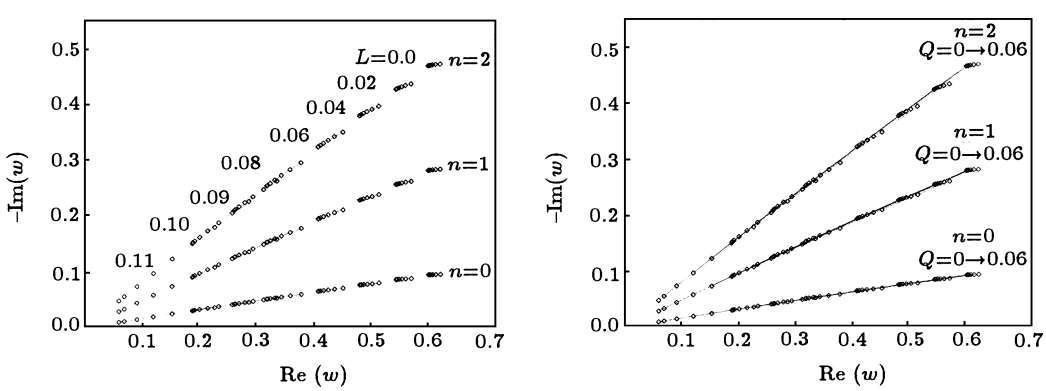


Fig.2. Gravitational QNMs for the axial perturbation: $l = 3$. In the left figure the curves are drawn for $\Lambda = L$=0, 0.02, 0.04, 0.06, 0.08, 0.09, 0.10, 0.11, and in the right figure the curves are drawn for Q=0, 0.1, 0.2, 0.3, 0.4, 0.5, 0.6.

Table 3. Gravitational quasinormal mode frequencies for the axial perturbation: $l = 5$.

ω	Q=0.0	Q=0.1	Q=0.2	Q=0.3	Q=0.4	Q=0.5	Q=0.6
				n=0			
$\Lambda = 0.00$	1.014–0.0951i	1.015–0.0951i	1.017–0.0952i	1.021–0.0953i	1.029–0.0955i	1.040–0.0957i	1.056–0.0960i
$\Lambda = 0.02$	0.9183–0.0863i	0.9191–0.0864i	0.9222–0.0865i	0.9279–0.0868i	0.9372–0.0875i	0.9507–0.0878i	0.9697–0.0884i
$\Lambda = 0.04$	0.8112–0.0764i	0.8124–0.0765i	0.8165–0.0768i	0.8239–0.0773i	0.8355–0.0780i	0.8519–0.0789i	0.8743–0.0799i
$\Lambda = 0.06$	0.6877–0.0649i	0.6894–0.0651i	0.6950–0.0653i	0.7048–0.0663i	0.7196–0.0674i	0.7401–0.0687i	0.7673–0.0704i
$\Lambda = 0.08$	0.5365–0.0508i	0.5391–0.0510i	0.5471–0.0517i	0.5610–0.0529i	0.5810–0.0546i	0.6080–0.0566i	0.6427–0.0591i
$\Lambda = 0.09$	0.4419–0.0419i	0.4453–0.0422i	0.4556–0.0431i	0.4729–0.0447i	0.4976–0.0468i	0.5298–0.0494i	0.5703–0.0526i
$\Lambda = 0.10$	0.3206–0.0304i	0.3256–0.0309i	0.3403–0.0322i	0.3643–0.0344i	0.3969–0.0374i	0.4378–0.0409i	0.4879–0.0450i
$\Lambda = 0.11$	0.1014–0.0096i	0.1170–0.0111i	0.1550–0.0147i	0.2042–0.0193i	0.2598–0.0245i	0.3205–0.0300i	0.3870–0.0358i
				n=1			
$\Lambda = 0.00$	1.014–0.2854i	1.015–0.2854i	1.017–0.2856i	1.021–0.2860i	1.029–0.2865i	1.040–0.2872i	1.056–0.2879i
$\Lambda = 0.02$	0.9183–0.2590i	0.9192–0.2591i	0.9222–0.2596i	0.9279–0.2605i	0.9372–0.2617i	0.9508–0.2633i	0.9697–0.2651i
$\Lambda = 0.04$	0.8112–0.2293i	0.8124–0.2295i	0.8165–0.2304i	0.8239–0.2319i	0.8355–0.2340i	0.8519–0.2367i	0.8743–0.2398i
$\Lambda = 0.06$	0.6877–0.1948i	0.6894–0.1952i	0.6950–0.1966i	0.7048–0.1989i	0.7196–0.2021i	0.7401–0.2062i	0.7673–0.2111i
$\Lambda = 0.08$	0.5365–0.1523i	0.5391–0.1530i	0.5471–0.1551i	0.5610–0.1587i	0.5810–0.1636i	0.6080–0.1699i	0.6427–0.1774i
$\Lambda = 0.09$	0.4419–0.1256i	0.4453–0.1265i	0.4556–0.1293i	0.4729–0.1340i	0.4976–0.1403i	0.5298–0.1483i	0.5703–0.1577i
$\Lambda = 0.10$	0.3206–0.0912i	0.3256–0.0926i	0.3403–0.0967i	0.3643–0.1033i	0.3969–0.1121i	0.4378–0.1227i	0.4874–0.1350i
$\Lambda = 0.11$	0.1014–0.0289i	0.1170–0.0333i	0.1550–0.0441i	0.2042–0.0580i	0.2598–0.0735i	0.3205–0.0900i	0.3870–0.1073i
				n=2			
$\Lambda = 0.00$	1.014–0.4756i	1.015–0.4757i	1.017–0.4760i	1.021–0.4767i	1.029–0.4776i	1.040–0.4787i	1.056–0.4798i
$\Lambda = 0.02$	0.9183–0.4316i	0.9192–0.4319i	0.9222–0.4327i	0.9279–0.4342i	0.9372–0.4362i	0.9508–0.4388i	0.9697–0.4418i
$\Lambda = 0.04$	0.8112–0.3821i	0.8124–0.3826i	0.8165–0.3840i	0.8239–0.3865i	0.8355–0.3900i	0.8519–0.3944i	0.8743–0.3997i
$\Lambda = 0.06$	0.6877–0.3246i	0.6894–0.3254i	0.6950–0.3276i	0.7048–0.3315i	0.7196–0.3368i	0.7401–0.3437i	0.7673–0.3519i
$\Lambda = 0.08$	0.5365–0.2538i	0.5391–0.2550i	0.5471–0.2586i	0.5610–0.2645i	0.5810–0.2727i	0.6088–0.2832i	0.6427–0.2957i
$\Lambda = 0.09$	0.4419–0.2093i	0.4453–0.2108i	0.4556–0.2156i	0.4729–0.2233i	0.4976–0.2339i	0.5299–0.2471i	0.5703–0.2628i
$\Lambda = 0.10$	0.3206–0.1520i	0.3256–0.1543i	0.3403–0.1612i	0.3643–0.1722i	0.3969–0.1868i	0.4378–0.2045i	0.4874–0.2249i
$\Lambda = 0.11$	0.1014–0.0481i	0.1170–0.0555i	0.1550–0.0735i	0.2042–0.0967i	0.2598–0.1223i	0.3205–0.1500i	0.3870–0.1789i
				n=3			
$\Lambda = 0.00$	1.014–0.6659i	1.015–0.6660i	1.017–0.6665i	1.021–0.6673i	1.029–0.6686i	1.040–0.6702i	1.056–0.6717i
$\Lambda = 0.02$	0.9183–0.6042i	0.9192–0.6046i	0.9222–0.6058i	0.9279–0.6078i	0.9372–0.6107i	0.9508–0.6144i	0.9697–0.6185i
$\Lambda = 0.04$	0.8112–0.5349i	0.8124–0.5356i	0.8165–0.5377i	0.8239–0.5411i	0.8355–0.5460i	0.8519–0.5522i	0.8743–0.5595i
$\Lambda = 0.06$	0.6877–0.4545i	0.6892–0.4555i	0.6950–0.4587i	0.7048–0.4641i	0.7196–0.4716i	0.7401–0.4811i	0.7673–0.4926i
$\Lambda = 0.08$	0.5365–0.3553i	0.5391–0.3570i	0.5471–0.3620i	0.5610–0.3703i	0.5810–0.3818i	0.6080–0.3965i	0.6427–0.4139i
$\Lambda = 0.09$	0.4419–0.2930i	0.4453–0.2952i	0.4556–0.3018i	0.4729–0.3126i	0.4976–0.3274i	0.5298–0.3460i	0.5703–0.3679i
$\Lambda = 0.10$	0.3206–0.2128i	0.3256–0.2160i	0.3403–0.2257i	0.3643–0.2411i	0.3969–0.2615i	0.4378–0.2863i	0.4874–0.3149i
$\Lambda = 0.11$	0.1014–0.0674i	0.1170–0.0777i	0.1550–0.1029i	0.2042–0.1353i	0.2598–0.1714i	0.3205–0.2100i	0.3870–0.2505i
				n=4			
$\Lambda = 0.00$	1.014–0.8561i	1.015–0.8563i	1.017–0.8569i	1.021–0.8580i	1.029–0.8596i	1.040–0.8616i	1.056–0.8636i
$\Lambda = 0.02$	0.9183–0.7769i	0.9192–0.7774i	0.9221–0.7789i	0.9279–0.7815i	0.9372–0.7852i	0.9508–0.7899i	0.9697–0.7952i
$\Lambda = 0.04$	0.8112–0.6878i	0.8124–0.6886i	0.8165–0.6913i	0.8239–0.6957i	0.8353–0.7020i	0.8519–0.7100i	0.8743–0.7194i
$\Lambda = 0.06$	0.6877–0.5843i	0.6894–0.5857i	0.6950–0.5898i	0.7048–0.5967i	0.7193–0.6063i	0.7401–0.6186i	0.7673–0.6333i
$\Lambda = 0.08$	0.5365–0.4568i	0.5391–0.4590i	0.5471–0.4654i	0.5610–0.4761i	0.5810–0.4909i	0.6080–0.5097i	0.6427–0.5322i
$\Lambda = 0.09$	0.4419–0.3767i	0.4453–0.3795i	0.4556–0.3880i	0.4729–0.4019i	0.4976–0.4210i	0.5298–0.4448i	0.5703–0.4730i
$\Lambda = 0.10$	0.3206–0.2736i	0.3256–0.2778i	0.3403–0.2901i	0.3643–0.3098i	0.3969–0.3362i	0.4378–0.3682i	0.4874–0.4049i
$\Lambda = 0.11$	0.1014–0.0866i	0.1170–0.0999i	0.1551–0.1323i	0.2042–0.1740i	0.2598–0.2204i	0.3205–0.2699i	0.3870–0.3220i

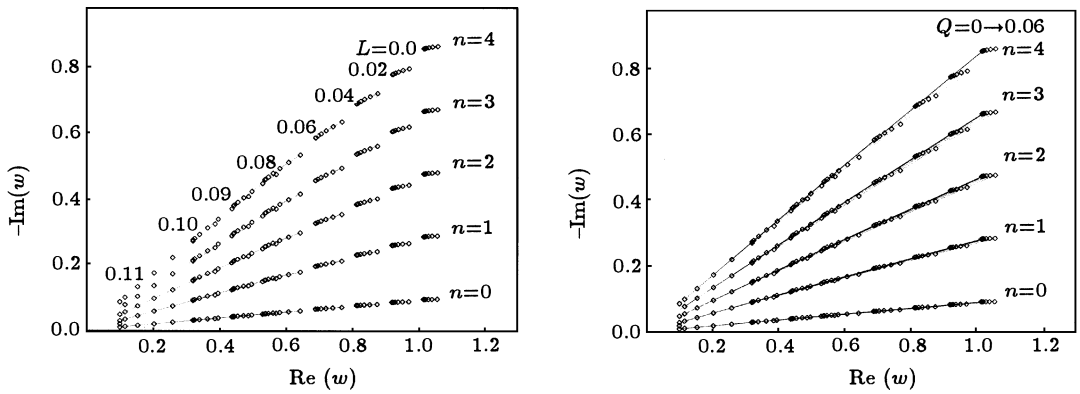


Fig.3. Gravitational QNMs for the axial perturbation: $l = 5$. In the left figure the curves are drawn for $\Lambda = L$=0, 0.02, 0.04, 0.06, 0.08, 0.09, 0.10, 0.11, and in the right figure the curves are drawn for Q=0, 0.1, 0.2, 0.3, 0.4, 0.5, 0.6.

We find that the gravitational quasinormal modes for the polar perturbation whose potential is described by Eq.(6) are exactly the same as those for the axial perturbation. Therefore, we list the results of the axial perturbation only. The facts prove that the quasinormal modes are fixed only by the parameters of the black hole and are independent of the initial perturbations.

We also check the calculations by using the 6th order WKB approximation, and find that the results obtained by the two methods are in very good agreement with each other, especially for the case of large cosmological constant or low overtone.

In the calculations we hold 85 digits in all intermediate values. All values are measured in the black hole mass units, $M = 1$.

3. Summary and discussion

The QNMs of the Reissner–Nordström de Sitter black hole for the axial and polar gravitational perturbations are investigated by using Pöschl–Teller approximation. It is shown that the magnitude of imaginary parts decreases as the cosmological constant increases, but it increases as the charge, or the overtone number or the orbital angular momentum increases. From the figures we learn that the imaginary part is almost linearly related to the real part as cosmological constant changes for a fixed charge. We also find that the gravitational QNMs of the Reissner–Nordström de Sitter black hole are the same for both the axial and polar perturbations, which indicates that the gravitational QNM frequencies are determined only by the mass M, the charge Q, and the cosmological constant Λ and are independent of the initial perturbations.

References

[1] Kokkotas K D and Schmidt B G 1999 *Living Rev. Rel.* **2** 2
[2] Nollert H P 2000 *Class. Quantum Grav.* **16** R519
[3] Frolov V P and Novikov I D 1998 *Black Hole Physics: Basic Concepts and New Developments* (Dordrecht: Kluwer)
[4] Chandrasekhar S and Detweller S 1975 *Proc. R. Soc. Lond.* A **344** 441
[5] Regge T and Wheeler J A 1957 *Phys. Rev.* **108** 1063
[6] Gundlach C, Price R H and Pullin J 1994 *Phys. Rev.* D **49** 883
[7] Burko L M and Ori A 1997 *Phys. Rev.* D **56** 7820
[8] Andersson N 1997 *Phys. Rev.* D **55** 468
[9] Hod S and Piran T 1998 *Phys. Rev.* D **58** 024017
[10] Hod S and Piran T 1998 *Phys. Rev.* D **58** 044018
[11] Leaver E 1986 *Phys. Rev.* D **34** 384
[12] Andersson N and Glampedakis K 2000 *Phys. Rev. Lett.* **84** 4537
[13] Hod S 1998 *Phys. Rev. Lett.* **81** 4293
[14] Berti E and Kokkotas K D 2003 *hep-th*/0303029
[15] Chan J S F and Mann R B 1997 *Phys. Rev.* D **55** 7546
[16] Birmingham D, Sachs I and Solodukhin S N 2002 *Phys. Rev. Lett.* **88** 151301
[17] Cardoso V and Lemos J P S 2001 *Phys. Rev.* D **63** 124015
[18] Konoplya R A 2002 *Phys. Rev.* D **66** 084007
[19] Starinets A O 2002 *Phys. Rev.* D **66** 124013
[20] Horowitz G T and Hubeny V E 2000 *Phys. Rev.* D **62** 024027
[21] Kurita Y and Sakagami M A 2003 *Phys. Rev.* D **67** 024003

[22] Cardoso V and Lemos J P S 2001 *Phys. Rev.* D **64** 084017
[23] Cardoso V, Konoplya R and Lemos J P S 2003 *gr-qc*/0305037
[24] Wang B, Lin C Y and Molina C 2004 *hep-th*/0407024
[25] Shen Z X, Wang B and Su R K 2004 *Chin. Phys. Lett.* **21** 428
[26] Konoplya R A 2002 *Phys. Rev.* D **66** 044009
[27] Moss I G and Norman J P 2002 *Class. Quantum Grav.* **19** 2323
[28] Cardoso V and Lemos J P S 2003 *Phys. Rev.* D **67** 084020
[29] Molina C 2003 *gr-qc*/0304053
[30] Maassen A 2003 *gr-qc*/0304092
[31] Suneeta V 2003 *gr-qc*/0303114
[32] Giammatteo M and Jiliang Jing 2004 *gr-qc*/0403030
[33] Zhidenko A 2003 *gr-qc*/0307012
[34] Perlmutter S *et al* 1997 *Astrophys. J* **483** 565
[35] Caldwell R, Dave R and Steinhardt P J 1998 *Phys. Rev. Lett.* **80** 1582
[36] Garnavich P M *et al* 1998 *Astrophys. J* **509** 74
[37] Jiliang Jing 2004 *Phys. Rev.* D **69** 084009
[38] Mellor F and Moss I G 1990 *Phys. Rev.* D **41** 403
[39] Leaver E W 1985 *Proc. Roy. Soc. Lon.* A **402** 285
[40] Ferrari V and Mashhoon B 1984 *Phys. Rev.* **30** 295